


A Purified Resin Glycoside Fraction from Pharbitidis Semen Induces Paraptosis by Activating Chloride Intracellular Channel-1 in Human Colon Cancer Cells

Integrative Cancer Therapies
18(1): 1–13
© The Author(s) 2019
Article reuse guidelines:
sagepub.com/journals-permissions
DOI: 10.1177/1534735418822120
journals.sagepub.com/home/ict


Dongrong Zhu, MD¹, Chen Chen, PhD¹, Yuanzheng Xia, PhD¹,
Ling-Yi Kong, PhD¹, and Jianguang Luo, PhD¹ 

Abstract

Pharbitidis Semen has worldwide recognition in traditional medicine for the treatment of several illnesses apart from its purgative properties, and it is also reported to show anticancer effect. However, limited pharmacological studies are available on the extract or resin glycosides fraction of Pharbitidis Semen. The purpose of this study was to determine the mechanism of the colon cancer cell cytotoxic effect of a purified resin glycoside fraction from Pharbitidis Semen (RFP). Our results showed that the RFP-induced cell death was mediated by the caspase-independent and autophagy-protective paraptosis, a type of cell death that is characterized by the accumulation of cytoplasmic vacuoles and mitochondria swelling. RFP significantly stimulated endoplasmic reticulum stress, inhibited proteasome-dependent degradation, and activated the MAPK signaling pathway in human colon cancer cell lines. Furthermore, we found that RFP activated chloride intracellular channel-1 (CLIC1) and increased the intracellular Cl⁻ concentration. Blockage of CLIC1 by DIDS (disodium 4,4'-diisothiocyanato-2,2'-stilbenedisulfonate hydrate) attenuated cell death, cytoplasmic vacuolization, and endoplasmic reticulum stress, suggesting that CLIC1 acts as a critical early signal in RFP-induced paraptosis. In conclusion, results obtained indicated that the cytotoxic effect of RFP in colon cancer cells was the outcome of paraptosis mediated by activation of CLIC1.

Keywords

Pharbitidis Semen, resin glycoside, paraptosis, CLIC1, cytoplasmic vacuolization

Submitted August 21, 2018; revised October 30, 2018; accepted November 29, 2018

Introduction

Colon cancer is the third leading cause of cancer death in both men and women.¹ Current treatment of this cancer generally employs surgery, neoadjuvant radiotherapy, and adjuvant chemotherapy.² Anticancer drug-induced apoptosis is one of the mechanisms most commonly utilized in cancer therapy; however, cancer cells may develop various adaptive or innate mechanisms.³ Hence, targeting several forms of non-apoptotic programmed cell death (PCD) has been considered as a new strategy for combating cancers.

Paraptosis is a form of non-apoptotic cell death characterized by a process of vacuolization that begins with the physical enlargement of the endoplasmic reticulum (ER) and mitochondria.^{4,5} It lacks apoptotic morphology and does not respond to caspase inhibitors.⁶ Furthermore, some

reports assert that paraptosis is also involved in new protein synthesis, proteasomal inhibition,⁷ and MAP kinase activation.⁸ Although the mechanisms underlying paraptosis, especially the signals responsible for triggering ER and mitochondria dilatation, have not yet been fully elucidated, they could be associated with reactive oxygen species (ROS) generation, or the disruption of internal Ca²⁺ or K⁺

¹Jiangsu Key Laboratory of Bioactive Natural Product Research and State Key Laboratory of Natural Medicines, School of Traditional Chinese Pharmacy, China Pharmaceutical University, Nanjing, People's Republic of China

Corresponding Authors:

Jianguang Luo and Ling-Yi Kong, China Pharmaceutical University, Nanjing 210009, People's Republic of China.
Email: luojg@cpu.edu.cn; cpu_lykong@126.com



ion homeostasis.⁹ Interestingly, another report showed that uptake of Cl^- may also be involved in cell swelling.¹⁰ The induction of paraptotic cell death is an alternative and emerging strategy to trigger cancer cell death, and exploiting apoptosis-independent PCD pathways may lead to the development of novel cancer therapies.

Natural products are valuable sources for the development of new anticancer drugs.^{11,12} Pharbitidis Semen, the seeds of *Pharbitis nil* (Convolvulaceae), is famous for its outstanding cathartic effect. In addition, it is also reported to have the antitumor effects.¹³ The prominent components of Pharbitidis Semen are resin glycosides.¹⁴ Resin glycosides are members of a very extensive family of secondary metabolites known as glycolipids. The complex resins are unique constituents of the morning glory family and they demonstrate various antitumor effects.¹⁵ For example, tricolorin A as the first individual resin glycoside has mammalian cytotoxicity.¹⁶ Cairicoside E, a natural resin glycoside compound isolated from *Ipomoea cairica*, was reported to have antimetastatic effect.¹⁷ Aquaterin II obtained from water spinach can inhibit HepG2 cell growth.¹⁸ However, limited pharmacological studies are available on the extract or resin glycosides of Pharbitidis Semen. Moreover, mechanism studies on the cytotoxic effect of resin glycosides from Pharbitidis Semen have not yet been documented, although it has medicinal value in cancer disease. In the present study, we investigated a purified resin glycoside fraction from Pharbitidis Semen (RFP) induction of paraptosis-like cell death and explored the underlying mechanisms.

Materials and Methods

Plant Material

Pharbitidis Semen, *Pharbitis nil* (L) Choisy, from the Convolvulaceae family, was purchased from Hebei Province of China in April 2014, and was authenticated by Professor Min-Jian Qin, Department of Medicinal Plants, China Pharmaceutical University. A voucher specimen (No. 2014-PBC) is deposited in the Department of Natural Medicinal Chemistry, China Pharmaceutical University. The authentication of the plant was alternatively confirmed through <http://www.theplantlist.org>.

Extraction and Isolation of the Purified Resin Glycoside Fraction (RFP)

The dried and powdered seeds of *P nil* (500 g) were extracted with ultrasonication in MeOH. After removal of solvent, the residue (47.1 g) was suspended in H_2O and successively extracted with petroleum ether (Fr. A), CH_2Cl_2 (Fr. B), EtOAc (Fr. D), and n-BuOH (Fr. E). Serious

emulsification appeared when extracted with CH_2Cl_2 , with no effective methods to break it. The emulsion layer was dissolved in MeOH (45 mL) with sonication for 10 minutes, then stood overnight to afford MeOH-soluble fraction (Fr. C, 14 g) and MeOH-insoluble fraction (Fr. C'). After various efforts attempting to isolate individual constituents from the MeOH-soluble fraction (Fr. C), our group identified 11 acylated resin glycosidic acid methyl esters by NH_2 silica gel-catalyzing methyl esterification of carboxylic acids in MeOH-soluble fraction (Fr. C)¹⁹ (Supplemental Figure S1, available online). Therefore, we characterized the MeOH-soluble fraction as a RFP and acylated glycosidic acid methyl esters compounds as RFP'.

Chemicals and Antibodies

MTT, calcein-AM, EthD-1, AnnexinV-FITC/PI, ER-tracker, Mito-Tracker, Fluo-4-AM, DAPI, Hoechst 33342, H2DCF-DA, MEQ, and BCECF-AM were purchased from Yeasen (Shanghai, China). Z-VAD-fmk, 3-methyladenine (3-MA), bafilomycinA1 (Baf), cycloheximide (CHX), *N*-acetylcysteine (NAC), reduced glutathione (GSH), SB203580, U0126, SP600125, ruthenium red (RR), and disodium 4,4'-diisothiocyanato-2,2'-stilbenedisulfonate hydrate (DIDS) were obtained from Selleck Chemicals (Houston, TX). The following antibodies were used: Cleaved Caspase Antibody Sampler Kit 9929T (cleaved caspase-3, -7, and -9 and cleaved poly-ADP-ribose polymerase [PARP]), Procaspase Antibody Sampler Kit 12742T (Caspase-3, -7, and -9; PARP), Bcl-2 (3498T), Bax (2772T), Beclin-1(3495T), LC3I/II (12741T), p62(5114S), ER Stress Antibody Sampler Kit 9956T (calnexin, BiP, IRE1 α , CHOP), ubiquitin (43124S), XBP1s (83418S), MAPK Family Antibody Sampler Kit 9926T (ERK 1/2, p38, JNK), Phospho-MAPK Family Antibody Sampler Kit 9910T (phospho-ERK1/2, phospho-p38, phospho-JNK, Rabbit IgG HRP, Mouse IgG HRP), GAPDH (5174S), and chloride intracellular channel-1 (CLIC1; 53424S) were purchased from Cell Signaling Technology (Danvers, MA). Alexa Fluor 647 AffiniPure Goat anti-Rabbit immunoglobulin G (IgG; H + L) (cat: FMS-RBaf64701) was obtained from FCMRCS (Nanjing, China).

Cell Culture

The human colon cancer cell lines HT-29 and HCT-116 were purchased from the Cell Bank of Shanghai Institute of Biochemistry and Cell Biology, Chinese Academy of Sciences (Shanghai, China). HT-29 and HCT-116 cells were cultured in RPMI-1640 and Dulbecco modified Eagle's medium, respectively, supplemented with 10% fetal bovine serum (GIBCO, USA), 100 U/mL penicillin, and 100 mg/mL streptomycin at 37°C with 5% CO_2 .

Cell Viability Assay

Cells (7×10^3 /well) were seeded into a 96-well culture plate for 24 hours. Then cells were incubated with or without serial dilutions of RFP for 12, 24, and 36 hours. After treatment, cell viability was measured by MTT assay. If required, the pan-caspase inhibitor Z-VAD-fmk (20 μ M), 3-MA (0.25 mM), Baf (20 nM), SB203580 (20 μ M), U0126 (20 μ M), SP600125 (20 μ M), RR (4 μ M), and DIDS (100 μ M) were added to cells 1 hour before RFP treatment. Since treatment of NAC (5 mM), GSH (5 mM), and CHX (20 μ M) would disturb the MTT assay, cell viability was assessed by double labeling of cells with 2 μ M calcein-AM and 4 μ M EthD-1.

Vacuolated Cells Observation

Cells (2×10^5 /well) were seeded into a 6-well culture plate for 24 hours and then treated with various concentration of RFP for 24 hours. Vacuolated cells were observed using light microscopy. Inhibitors involved in the experiments were added 1 hour before RFP treatment.

Transmission Electron Microscopy

The ultra-structure of cytoplasmic vacuolization was observed using a Philips Tecnai-12 Biotwin transmission electron microscopy (TEM) similar to previous reports. Briefly, collected cells were fixed with 2% glutaraldehyde for 2 hours, washed with phosphate-buffered saline (PBS), and then post-fixed with 1% OsO₄ for 1.5 hours at 48°C. The samples were then washed and dehydrated with graded alcohol. After dehydration, the samples were infiltrated and embedded in 618 epoxy resin. Ultrathin sections were cut, stained with uranyl acetate and lead citrate, and then examined under the TEM.

Flow Cytometry Analysis

To detect apoptotic cells, ROS, and cytosolic free Ca²⁺, flow cytometry analysis was performed according to the manufacturer's instructions. Apoptotic cells were measured using an AnnexinV-FITC/PI apoptosis detection kit. Cells were collected and washed with PBS before staining for 15 to 30 minutes at 37°C, and then analyzed by flow cytometry. ROS and cytosolic free Ca²⁺ detection were the same as apoptosis except washing 3 times with HBSS after staining with corresponding fluorescence probe Fluo-4AM or H2DCFDA.

ER and Mitochondria Localization

ER or mitochondria staining were performed according to the instructions of the manufacturer of ER-tracker or Mito-tracker kits. Briefly, RFP-treated cells were washed with HBSS (containing Ca²⁺ and Mg²⁺) and then incubated in prewarmed ER-tracker (1 μ M) or Mito-tracker (20 nM) combined with Hoechst 33342 (5 μ M) for 30 minutes at

37°C. After washing with HBSS, the cells were observed using Image Xpress Micro Confocal ($\times 60$).

Immunocytologic Staining

Staining of intracellular CLIC1 and ER membrane protein calnexin were conducted using immunofluorescence. Briefly, after RFP treatment, cells were washed with PBS and then fixed for 15 minutes at room temperature with 4% paraformaldehyde and permeabilized with 0.2% Triton X-100 in PBS for 10 minutes, followed by PBS washes. Unspecific binding was blocked with 5% bovine serum albumin (BSA) for 1 hour at room temperature. Cells were then incubated overnight at 4°C with primary antibody (rabbit anti-CLIC1 or anti-calnexin polyclonal antibody in 5% BSA). After PBS washes, cells were incubated with Alexa Fluor 647-conjugated secondary antibody for 1 hour in the dark. After additional PBS washes, cells were observed using Image Xpress Micro Confocal.

Visualization of Intracellular Ca²⁺, Cl⁻, and pH

To determine intracellular Ca²⁺, Cl⁻, and pH level after RFP treatment, we applied fluorescence probes Fluo-4 AM, MEQ, or BCECF-AM to visualize the Ca²⁺, Cl⁻, and pH. After treatment with or without RFP for 24 hours, cells were stained for 20 minutes at 37°C and then washed with HBSS for 3 times. Finally, the cells were imaged by Image Xpress Micro Confocal.

Western Blot

Cells with different treatments were washed twice with PBS, then collected and lysed in western IP buffer. The cell lysates were separated on sodium dodecyl sulfate polyacrylamide gels and transferred to polyvinylidene difluoride membranes. After blocking nonspecific binding with TBS-T containing 5% nonfat milk for 1 hour at room temperature, the membranes were immunoblotted with the primary antibodies at 4°C overnight. Then the membranes were incubated with HRP-conjugated goat anti-rabbit or anti-mouse secondary antibody for 2 hours at room temperature. The protein bands were detected using the ChemiDOC system (Bio-Rad, Hercules, CA).

Statistical Analysis

All data were presented as mean \pm SD from at least 3 separate experiments. Student's *t* test was applied to evaluate the differences between treated and control groups with cell viability. Data from multiple groups were analyzed by 1-way ANOVA (analysis of variance), followed by Bonferroni multiple comparison test. For all the tests, the level of significance was **P* < .05, ***P* < .01, ****P* < .001.

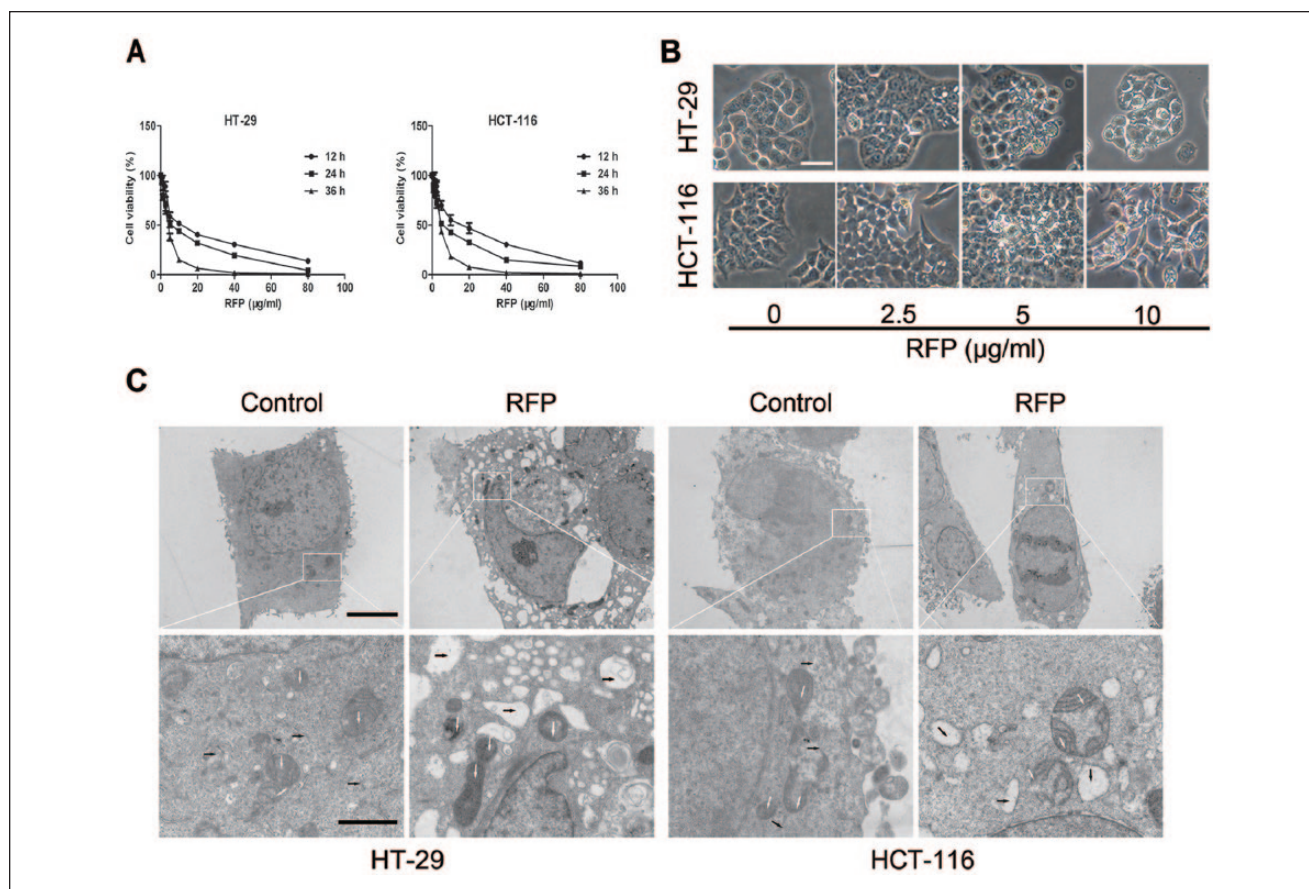


Figure 1. RFP demonstrated potent cytotoxic effects on colorectal cancer cells. (A) Cells were treated with RFP at the indicated concentrations for 12, 24, and 36 hours. Their cellular viabilities were assessed by MTT. (B) Light micrograph images ($\times 400$ magnification) of these cancer cells with indicated concentrations of RFP or without RFP treatment. Bar = 20 μm . (C) Electron microscopy ($\times 10\,000$ magnification) showing ultrastructure of cells untreated and treated with 5 $\mu\text{g}/\text{mL}$ RFP for 24 hours. White and black arrows represent mitochondria and cytoplasmic vacuoles, respectively. Bars, 5 μm and enlarged images, 1 μm .

Results

RFP Demonstrated Potent Cytotoxic Effects on Colorectal Cancer Cells

To examine the effect of several fractions of *Pharbitidis Semen* extraction on colon cancer cell viability, MTT assay was used. Interestingly, results obtained indicated that only RFP (Fr. C) potently inhibited cell growth and RFP', the acylated glycosidic acid methyl ester product of RFP, showed no cytotoxicity (Supplemental Table S1). RFP induced colon cancer cells in a time- and concentration-dependent manner. The IC_{50} values of RFP were 6.8 ± 1.6 $\mu\text{g}/\text{mL}$ in HT-29 cells and 6.3 ± 1.7 $\mu\text{g}/\text{mL}$ in HCT-116 cells (Figure 1A). Moreover, extensive intracellular vacuole surrounding the cell nucleus could be detected before cell death under light microscope after RFP treatment (Figure 1B). The RFP-induced cytoplasmic vacuolization was further observed by TEM (Figure 1C). Similar to the optical microscope imaging results, but more clearly, the high-magnification TEM image showed that most

of the intracellular vacuoles had irregular shapes and lacked a distinguishable double-layered membrane (black arrows), suggesting that they were not lysosomes or autophagosomes.

RFP Induced Paraptosis-Like Cell Death

To investigate whether RFP-induced cell death was associated with apoptosis, we examined the activation of caspases and downstream PARP protein levels. As a result of treatment for 24 hours, procaspase-3, -7, and -9 and PARP protein levels were not altered, and cleaved caspase-3, -7, and -9 and PARP proteins were detected at very low levels. Moreover, the protein expressions of BCL-2 and Bax were not affected by RFP treatment (Figure 2A). When the cells were pretreated with the broad-spectrum pan-caspase inhibitor Z-VAD-fmk before treatment with RFP, the percentage of dead cells (Figure 2B) and the cytoplasmic vacuolization (Figure 2C) were not rescued. To further confirm the types of RFP-induced cell death, AnnexinV/PI staining assay was

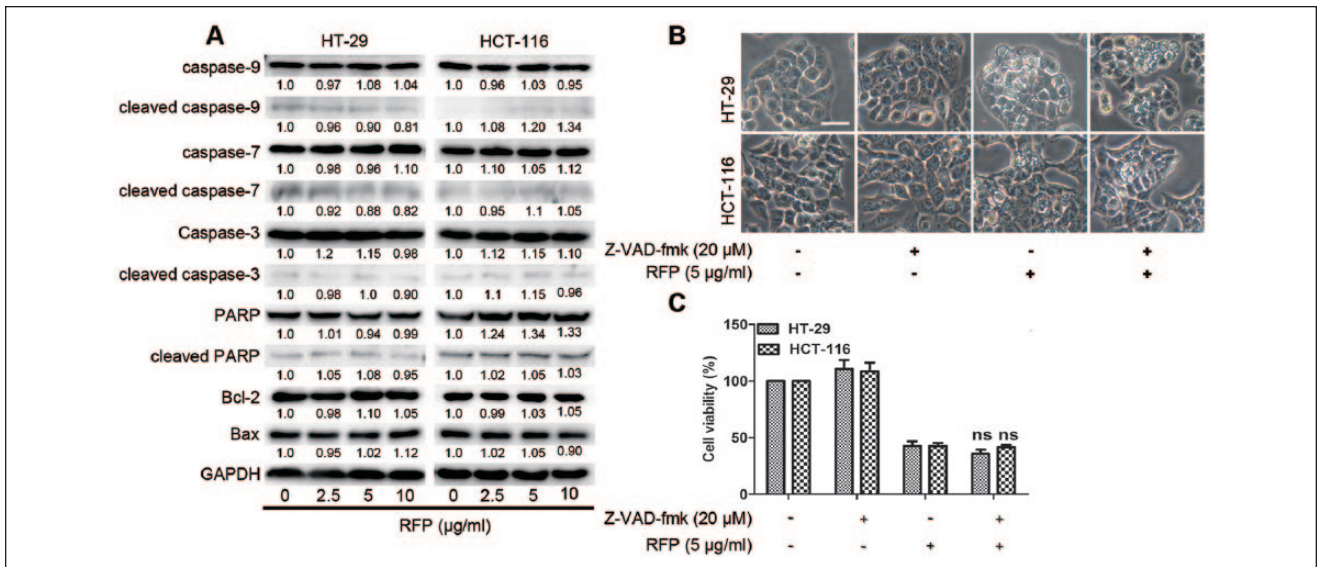


Figure 2. RFP induced paraptosis-like cell death. (A) Cells were lysed after treatment with RFP for 24 hours, and the apoptosis-related protein levels were detected by western blot analysis. GAPDH was used as an equal loading control. (B and C) Cells were pretreated with Z-VAD-fmk at 20 µM for 1 hour before treatment of RFP at 5 µg/mL for 24 hours. (B) Cell viability was measured by MTT assay. (C) Cells were imaged by light microscope. Bars, 20 µm.

applied to assess the extent of phosphatidyl-serine externalization and the disruption of the cell membrane. There was no clear change in the percentages of AnnexinV- or PI-positive cells between control and RFP-treated group (Supplemental Figure S2), ruling out apoptosis and necrosis as potential modes of RFP-induced cell death. Paraptosis is typically characterized as cytoplasmic vacuolization, not involving activation of caspases or insensitive to caspase inhibitors.⁶ Therefore, RFP-induced paraptosis-like cell death in colon cancers.

Autophagy Antagonized Paraptosis in RFP-Treated Colon Cancer Cells

To study the effect of RFP on autophagy in colon cancer, ultrastructural analysis by TEM revealed an increased number of autophagosomes in RFP-treated cells (Figure 3A). At the same time, the autophagy-related proteins were examined. The upregulation of beclin 1, the conversion from LC3I to LC3II, and the downregulation of p62 were detected in RFP treated cells in a concentration-dependent manner (Figure 3B). These results demonstrate that RFP induced autophagy in colon cancer cells. To further determine the role of autophagy in RFP-induced cell death, autophagy inhibitors 3-MA and Baf were applied. The level of autophagy-related proteins was blocked by autophagy inhibitors (Supplemental Figure S3). However, the cytoplasmic vacuolization and cell death were enhanced significantly by 3-MA and Baf (Figure 3C and D). Taken together, cytoplasmic vacuolization and cell death induced by RFP were

nonautophagic and autophagy antagonized paraptosis in colon cancer. This phenomenon was consistent with previous report that some reagents induced paraptosis and protective autophagy.^{6,20}

RFP Induced Cytoplasmic Vacuolization Originated From the ER and Mitochondria

From the TEM (Figure 1C), the vacuoles and swelling mitochondria appeared clear and no cytoplasmic material was observed in the vacuoles. To characterize the morphological changes of the cells treated with RFP, experiments were performed on cells by using ER-tracker, Mito-tracker staining, or ER membrane protein calnexin immunofluorescence (Figure 4A). Vacuoles and enlarged mitochondria could be observed through ER and mitochondria staining in colon cancer cells treated with RFP. ER membrane immunofluorescence also showed dilation of ER. These results indicated that cytoplasmic vacuoles induced by RFP might be dilated ER and mitochondria. In fact, ER vacuolization and enlarged mitochondria have been reported to be the typical features of paraptosis.^{4,5}

Since massive vacuoles were derived from the ER and inhibition of proteasomal activity was also involved in paraptosis,⁷ we measured the expression of certain ER resident proteins associated with protein folding and ubiquitinated proteins. Immunoblot analysis of the cells demonstrated that RFP upregulated the protein expressions of ER-stress markers glucose-regulated protein BiP/GRP78, C/EBP-homologous protein CHOP, IRE1α, the splicing of X-box

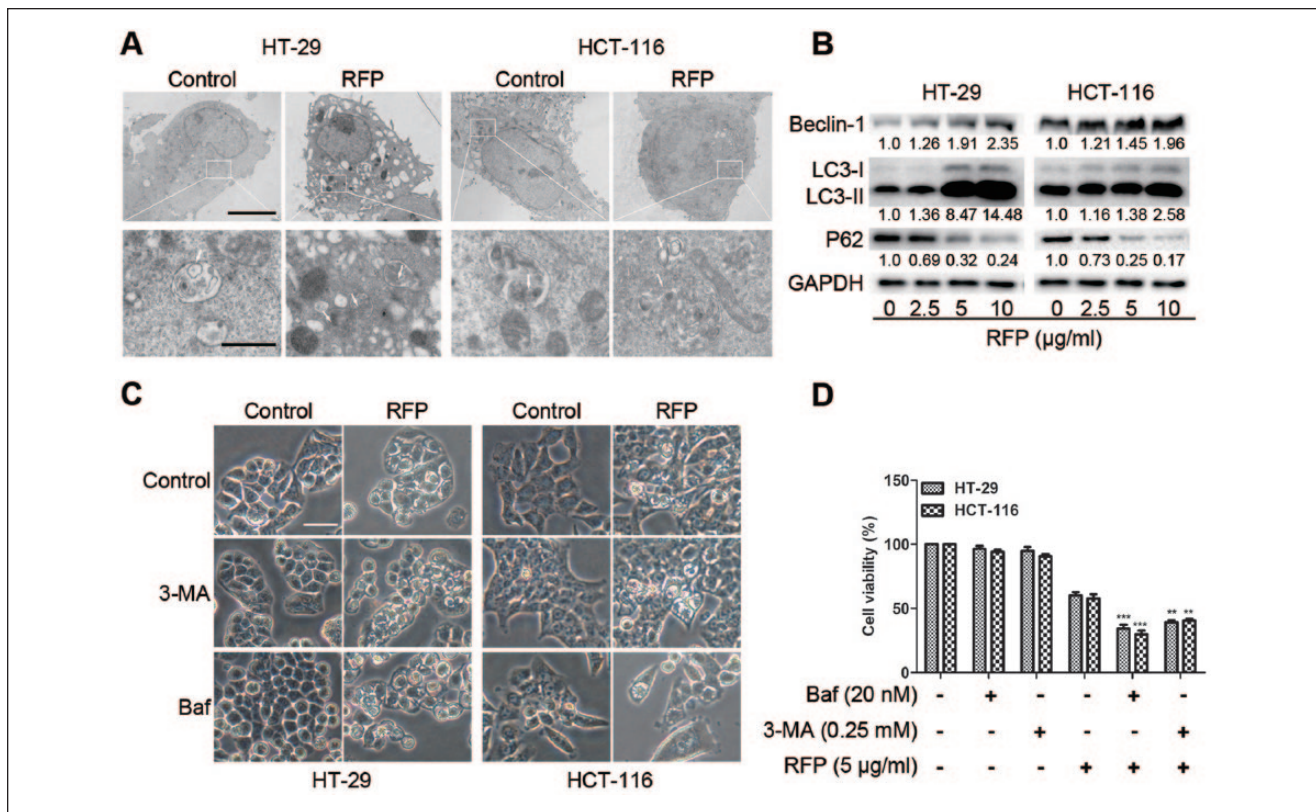


Figure 3. Autophagy antagonized paraptosis in RFP-treated colon cancer cells. (A) Cells were untreated or treated with 5 µg/mL RFP for 24 hours, and formation of autophagic vacuoles was examined by TEM analysis. White arrows represent double-membrane autophagosome. Bars, 5 µm, and enlarged images, 1 µm. (B) Cells were lysed after treatment with indicate concentration RFP for 24 hours, and the protein levels of beclin I, LC3II/I, and p62 were detected by western blot analysis. GAPDH was used as an equal loading control. (C) The cytoplasmic vacuolization was visualized by light microscope. Bars, 20 µm. (D) The cell viability was detected by MTT assay. ** $P < .01$, *** $P < .001$ versus cells treated with RFP alone.

binding protein 1s, and ubiquitinated proteins in a concentration and time-course manner (Figure 4B and Supplemental Figure S4). Collectively, the IRE1 branch of unfolded protein response signaling was activated and proteasome-dependent degradation was inhibited by RFP.

Furthermore, ongoing protein synthesis is required for paraptosis.²¹ To determine the impact of RFP on this function, we explored the role of protein synthesis in paraptosis using CHX as an inhibitor. As a result, the interruption of protein synthesis alleviated the formation of vacuoles (Figure 4C), ER stress (Figure 4D), and cell death (Figure 4E), suggesting that protein synthesis was necessary for this process, another characteristic of paraptosis.

RFP Activated MAPK Pathways in a Concentration- and Time-Dependent Manner

As MAP kinases have been positively associated with paraptosis,²² the activities of MAP kinase were examined after cell treatment with RFP. There was no clear change of the expression of p38, while the activities of JNKs and

ERKs were significantly increased in a concentration- and time-dependent manner (Figure 5A and Supplemental Figure S5). A further experiment was designed to test the functional significance of MAP kinases in cytoplasmic vacuolization and cell death. Observed results showed that cytoplasmic vacuolization and cell death were not rescued by inhibition of p38 activity with SB203580, but were significantly decreased by pretreatment with JNK and ERK inhibitors, SP60012 and U0126 (Figure 5B and C). These results indicated that JNKs and ERKs positively regulated RFP-induced cytoplasmic vacuolization and cell death.

The Paraptosis Induced by RFP Was Independent of ROS Generation or Intracellular Calcium Homeostasis

In previous reports, ROS generation or disruption of intracellular Ca^{2+} homeostasis were the early signals of paraptosis.⁹ Therefore, the effect of RFP on ROS generation was tested. Flow cytometry analysis using H2DCF-DA demonstrated that ROS levels were markedly increased

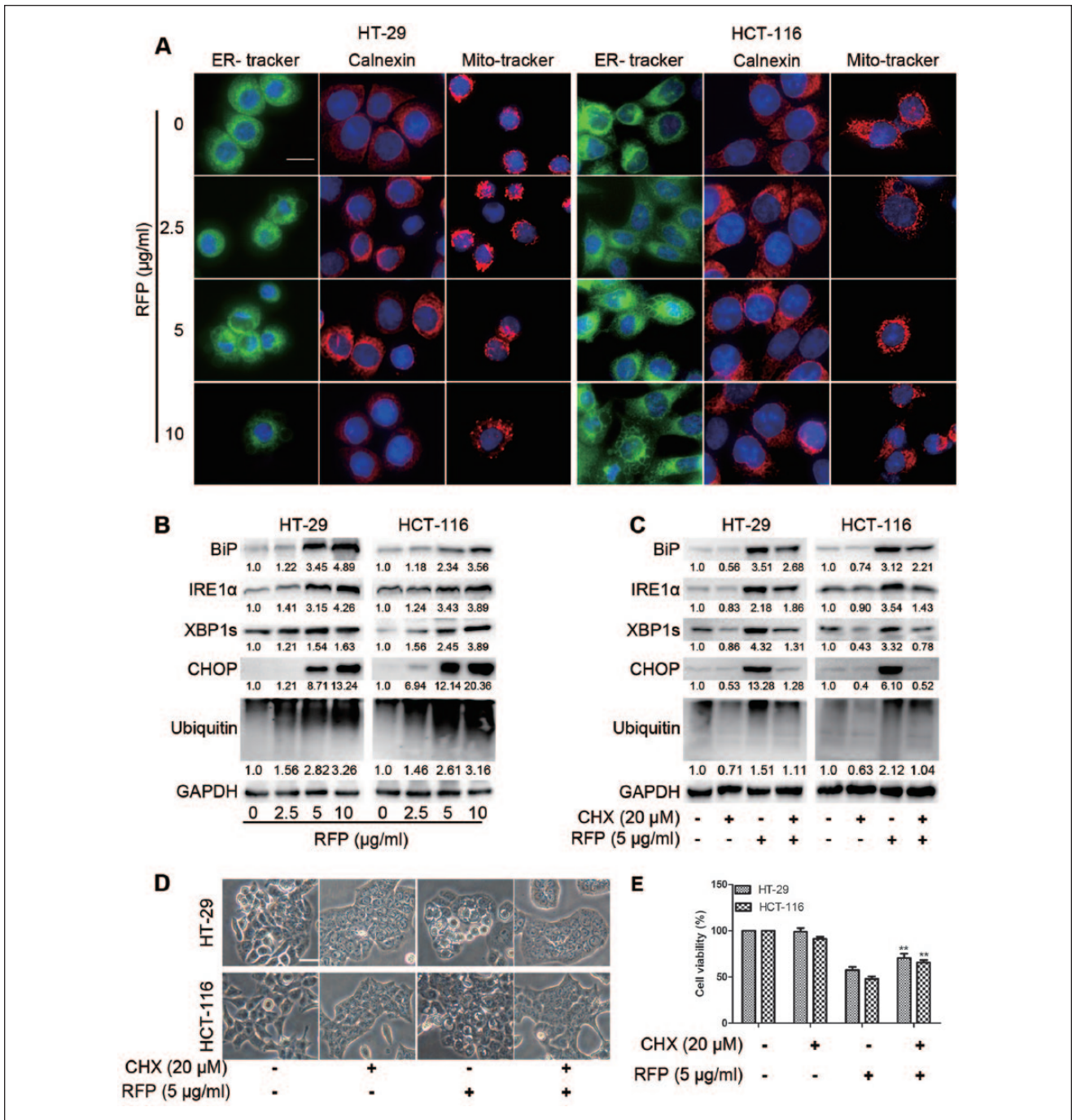


Figure 4. RFP induced cytoplasmic vacuolization originated from the ER and mitochondria. (A) Cells incubated with different concentration RFP for 24 hours then stained with ER-tracker, Mito-tracker, or staining calnexin that was embedded in the ER membrane and observed by ImageXpress Micro Confocal (×60). Bars, 20 µm. (B) Colon cancer cells were treated with indicated concentrations of RFP, and cell extracts were prepared for Western blot. (C-E) Cells were pretreated with CHX (20 µM, 1 hour), then treated with RFP at 5 µg/mL for 24 hours. (C) Cells were lysed for immunoblotting. (D) The vacuolated cells were measured using a light microscope. Bars, 20 µm. (E) Cell viability was detected using calcein-AM and EthD-1. ****P* < .001 versus cells treated with RFP alone.

after treatment cells with RFP in a concentration-dependent manner (Figure 6A). Next, we pretreated cells with antioxidants NAC or GSH and then exposed the cells to

5 µg/mL RFP for 24 hours. Interestingly, the same as the cytoplasmic vacuolization (Figure 6B) and cell death (Figure 6C), the response of unfolded protein response

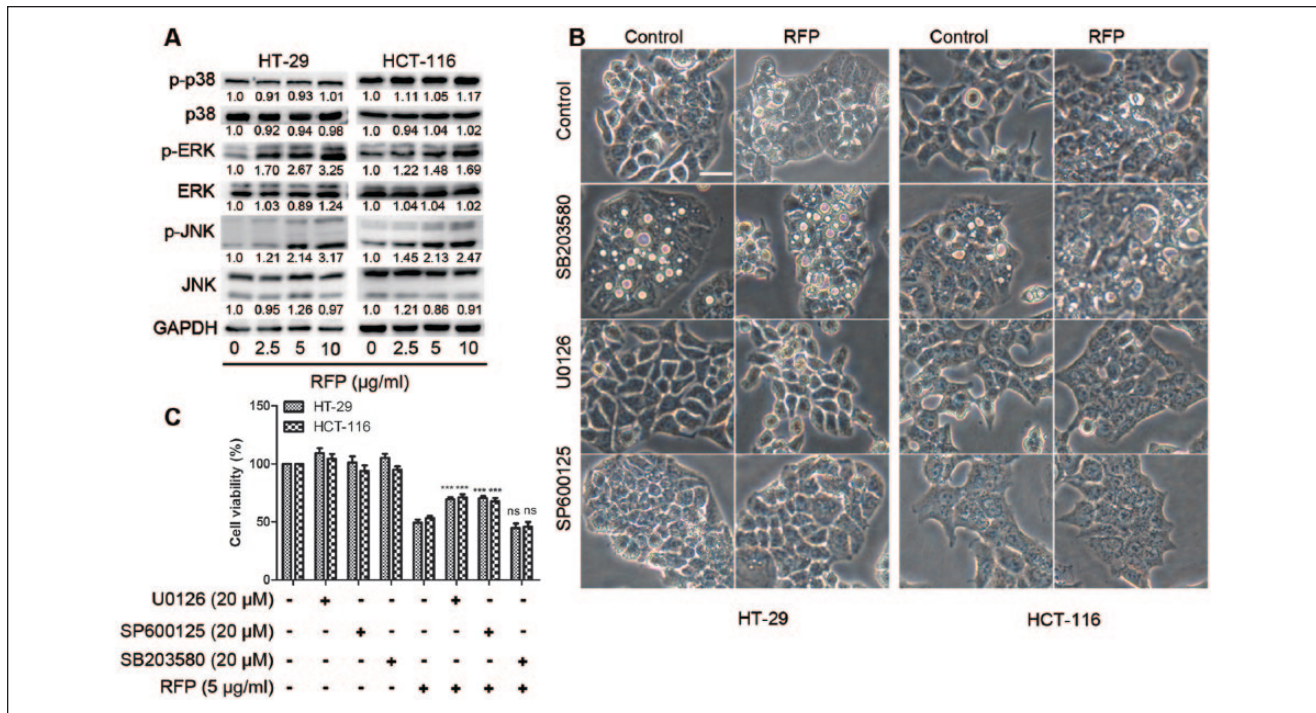


Figure 5. RFP Activated MAPK pathways in a concentration- and time-dependent manner. (A) Western blot of MAP kinases in cells treated with indicate concentrations of RFP. (B and C) Effects of the specific inhibitors of MAPK pathways on RFP-induced cellular dilation. Cells were pretreated with 20 µM SB203580, 20 µM SP600125, or 20 µM U0126 and further treated with 5 µg/mL RFP for 24 hours. (B) Treated cells were observed under the light microscope. Bars, 20 µm. (C) Cell viability was detected by MTT assay. ****P* < .001 versus cells treated with RFP alone.

and the level of ubiquitinated proteins was increased by antioxidants (Supplemental Figure S6). These results suggested that ROS generation was not responsible for paraptosis and on the contrary rescued the cell death.

Next, we determined the intracellular Ca^{2+} concentration with RFP treatment using Fluo-4AM by flow cytometry analysis. There was no significant difference in intracellular Ca^{2+} concentration (Figure 6D), consistent with the result of the confocal images (Supplemental Figure S7). RR, a Ca^{2+} uptake inhibitor, also could not suppress the forming of vacuoles and cell death (Figure 6E and F). All the results confirmed that RFP-induced vacuolization and cell death were not related to intracellular calcium homeostasis.

CLIC1 Activation Triggered RFP-Induced Paraptosis

Resin glycosides have amphiphilic structures that are easy to insert into biological membranes and their cytotoxic properties could be the result of a possible ion flux perturbation in the target cell membrane induced by nonselective pore formation.¹⁶ In addition, resin glycosides were reported to show the ability to increase the membrane permeability for both cations (K^+ and Na^+) and anions (Cl^-)

in a dose-dependent fashion.²³ RFP was a purified resin glycoside fraction, in which the free carboxyl groups of resin glycosides would change the cytoplasmic pH. CLIC1, a Cl^- channel sensitive to intracellular pH, could regulate cell volume and swelling,¹⁰ and might be associated with RFP-induced paraptosis. BCECF-AM, MEQ, and CLIC1 antibodies were used to measure intracellular pH, Cl^- concentration, and the expression of CLIC1. As shown in Figure 7A, a gradient alteration of fluorescence intensity was detected. Confocal images revealed that RFP decreased the intracellular pH, and elevated the concentration of cytoplasmic Cl^- and the expression of CLIC1. A following immunoblot further confirmed the upregulation of CLIC1 (Figure 7B). To determine the role of CLIC1 in RFP-induced paraptosis, DIDS, an inhibitor of CLIC1, was added before RFP treatment. We found that DIDS notably blocked the activation of CLIC1, decreased the Cl^- accumulation into cells, and improved the pH of cytoplasm (Figure 7C). More important, the cell death and cytoplasmic vacuolization were almost completely reversed by DIDS (Figure 7D and E). In addition, the activation of ERKs, JNKs, accumulation of polyubiquitinated proteins, and ER stress responses were blocked by DIDS (Figure 7F). These results indicated that CLIC1 played a

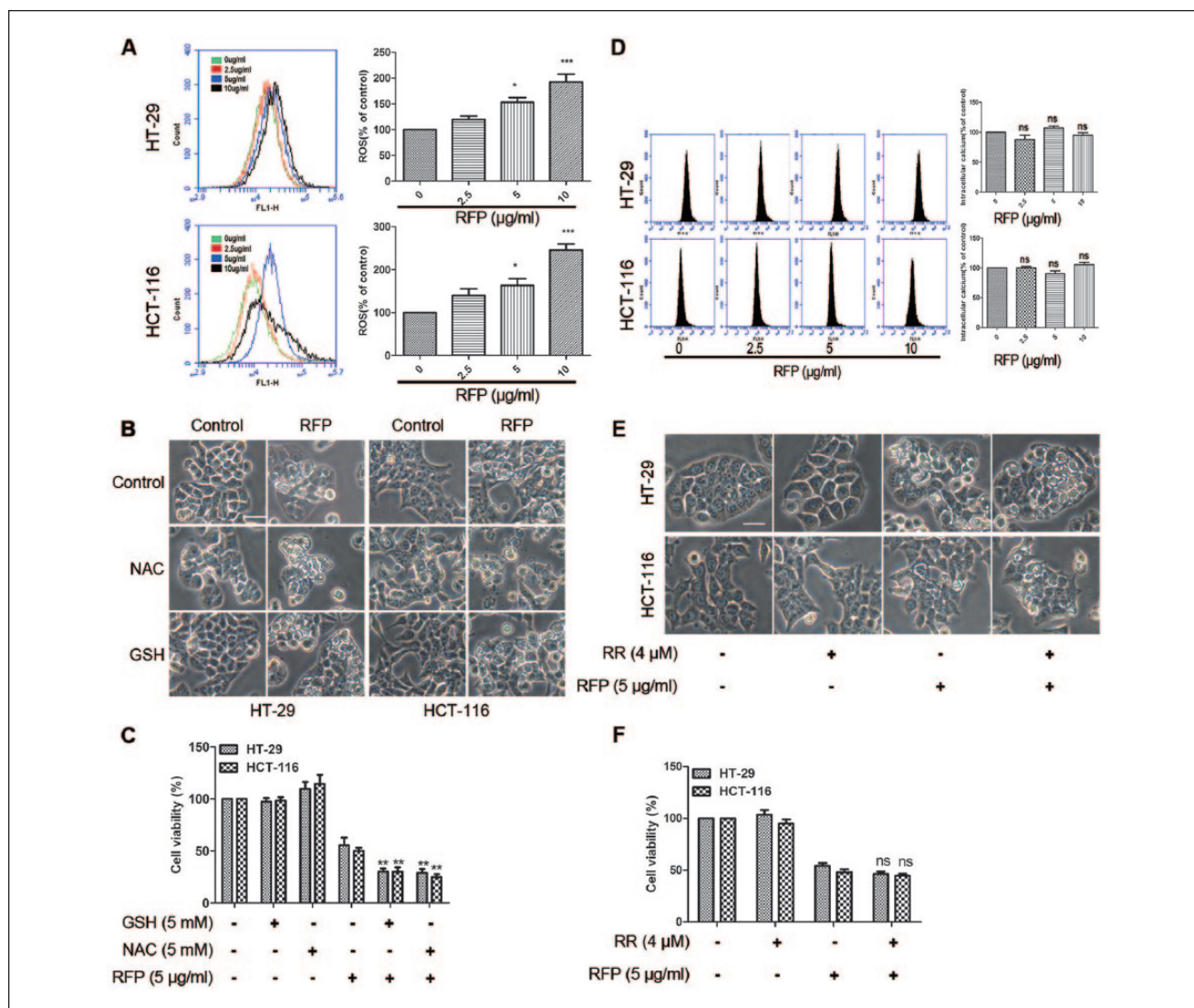


Figure 6. The paraptosis induced by RFP was independent of ROS generation or intracellular calcium homeostasis. (A) Cells were treated with RFP for different concentrations for 24 hours. The detection of ROS production in the treated cells is described in the “Materials and Methods” section. (B and C) Colon cancer cells were pretreated with ROS scavenger (NAC and GSH, 5 mM) alongside compounds treatment. (B) The microscopic images show ED the influence of ROS scavenger on cytoplasmic vacuole formation. Bars, 20 μm . (C) Cell viability was assessed using calcein-AM and EthD-1. $^{**}P < .01$ versus cells treated with RFP alone. (D) Cells were treated with indicated concentrations of RFP, then flow cytometry analysis was used to measure the intracellular Ca^{2+} concentration applying the Fluo-4AM fluorescence probe. (E and F) Ca^{2+} uniporter inhibitor RR (4 μM) was applied 1 hour before RFP treatment. (E) Cells were imaged by light microscope. Bars, 20 μm . (F) Cell viability was detected by MTT assay.

critical role in RFP-induced paraptosis. To further confirm that CLIC1 was an early signal of paraptosis, we applied the inhibitor of ERKs or JNKs and detected the expression of CLIC1. As shown in Figure 7G, the RFP-induced upregulation of CLIC1 was not blocked by pretreatment with ERK or JNK inhibitors, instead slightly increasing the expression. Altogether these data suggested that the RFP-induced anticancer effects were attributed to, at least in part, the modulation of Cl^- transport across the plasma membrane due to the modulation of CLIC1.

Discussion

It is reported that resin glycosides (the characteristic constituents of the plant in the Convolvulaceae family) have cytotoxic properties as their amphipathic moieties could perturb cell membranes through nonselective pore formation.^{15,16} Pharbitidis Semen is used as a traditional herb in Korea, China, and Japan. Resin glycosides were reported to be responsible for its pharmacologic effect.¹⁴ However, previous investigations on its crude resin glycosides only

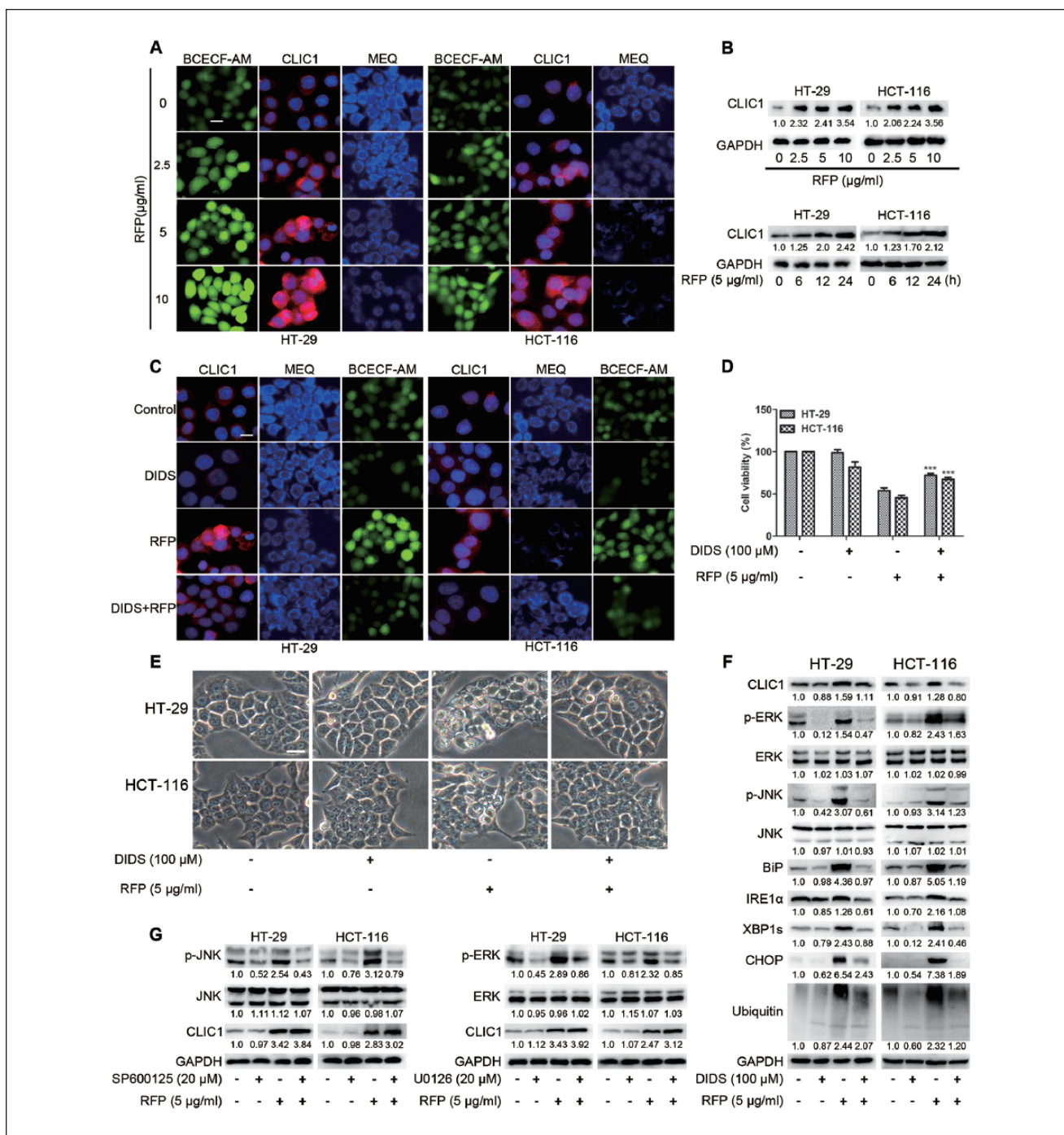


Figure 7. CLIC1 activation triggered RFP-induced paraptosis. (A) Image Xpress Micro Confocal ($\times 60$) imaged of intracellular pH, Cl^- , and CLIC1 antibody stained RFP treatment cells which indicate concentrations. Bars, 20 μm . (B) Immunoblot analysis of the expression of CLIC1 in cells after treatment with RFP. (C-F) Cells were pretreated with DIDS (100 μM) for 1 hour before treatment with or without RFP (5 $\mu\text{g/ml}$) for 24 hours. (C) Cells were stained with CLIC1 antibody, MEQ and BCECF-AM, then imaged by Image Xpress Micro Confocal. (D) Cell viability was detected by MTT assay. $***P < .01$ versus cells treated with RFP alone. (E) Cells were observed via optic microscopy. Bars, 20 μm . (F) Cell extracts were prepared for western blot. (G) Cells were pretreated with 20 μM SP600125, or 20 μM U0126 and further treated with 5 $\mu\text{g/ml}$ RFP for 24 hours. The CLIC1 was detected by immunoblot analysis.

characterized the glycoside acids or organic acids as alkaline hydrolysis products. The existence a free β -hydroxyl acid moiety resulting in the poor resolution hampered the

isolation of individual constituents.²⁴ Besides, intact structures were disclosed by derivatization using indium(III) chloride in methanol.²⁵ Recently, our group identified 11

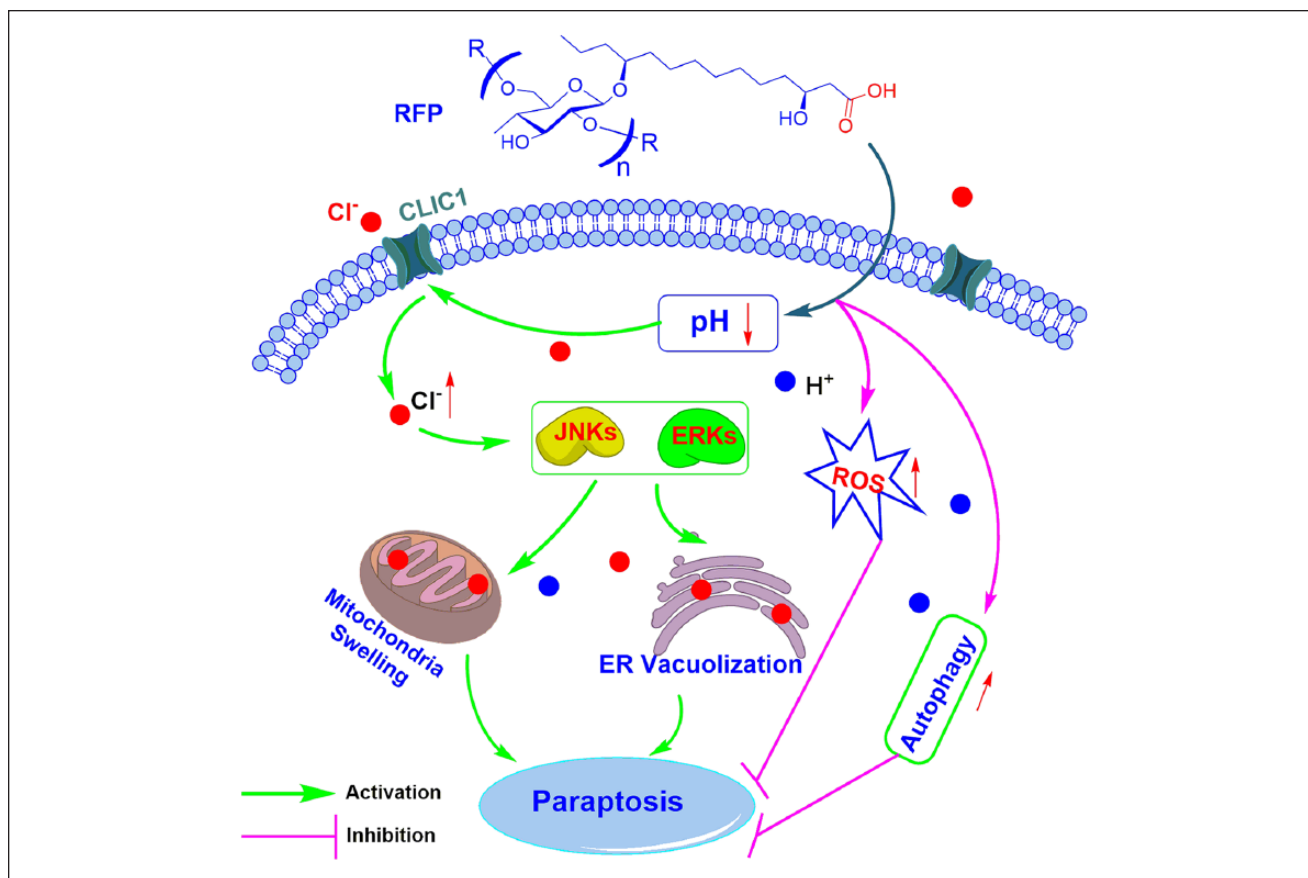


Figure 8. The proposed model of molecular interaction to delineate the action mechanisms of RFP in colon cancer cells.

acylated glycosidic acid methyl esters by NH_2 silica gel-catalyzing methyl esterification of carboxylic acids in RFP.¹⁹ Therefore, glycosidic acids were considered to be the main constituents of RFP. Interestingly, the RFP showed significant cytotoxicity while the acylated glycosidic acid methyl ester product of RFP exhibited no cytotoxicity, indicating that the glycosidic acids were the active constituents and the free carboxyl acid was the bio-active group.

In the present study, we found for the first time that RFP exhibited potent ability for inhibiting colorectal cancer cell growth and could induce extensive cytoplasmic vacuolization originated in the ER and mitochondria dilation. The vacuoles could be inhibited by MAPK inhibitors and translation inhibitor. More important, compared with paraptosis induced by previously reported reagents,^{22,26} RFP-induced paraptosis showed its own specific characteristics. On one hand, autophagy could be observed in cells treated with RFP. However, autophagy inhibitors aggravated RFP-induced cell death. On the other hand, apoptosis and necrosis ruled out RFP-induced cell death. Therefore, paraptosis played a crucial role in RFP-induced cell death and autophagy as a mechanism of cell survival that rescued cell death.

Previous studies demonstrated that ROS generation or the disruption of intracellular Ca^{2+} homeostasis was the initiating event of paraptosis.²⁶ We found that the ROS indeed were produced when treating cells with RFP; however, the ROS inhibitors could not block the cytoplasmic vacuolization and cell death, and on the contrary amplified the formation of vacuoles and ER stress. Interestingly, these results were similar to ginsenoside Rh2, which was reported to generate ROS via activating NF- κ B pathway to rescue cell death.²⁷ Besides, there was no significant difference of the intracellular Ca^{2+} concentration after RFP treatment (Figure 6). Thus, Ca^{2+} overload was excluded as an initial signal for RFP-induced paraptosis.

Several authors have suggested that regulation of the chloride conductance could be one means of regulating intracellular pH.²⁸ Another research showed that the chloride channels are required for cell volume regulation and acidification of intracellular organelles.¹⁰ Additionally, resin glycosides were reported to show the ability to increase the membrane permeability for anions (Cl^-) in a dose-dependent fashion.²³ Therefore, the proposed mechanism of RFP causing death in colon cancer cells by paraptosis is presented in Figure 8. RFP decreased intracellular

pH, which activated CLIC1, leading to a rapid increase in cell Cl^- content. The Cl^- dysregulation led to cell swelling and activated MAPK pathway to positively regulate paraptosis. Ultimately, accumulation of ER vacuolization and mitochondria swelling contributed to the induction of paraptosis-like cell death. Thus, our present study not only provides a new molecular insight into the mechanisms of paraptosis but also suggests a novel therapeutic strategy for inducing paraptosis in colon cancer cells.

The datasets analyzed during the current study are available from the corresponding author on reasonable request.

Declaration of Conflicting Interests

The author(s) declared no potential conflicts of interest with respect to the research, authorship, and/or publication of this article.

Funding

The author(s) disclosed receipt of the following financial support for the research, authorship, and/or publication of this article: This work was supported financially by the National Natural Science Foundation of China (No. 81573570), the Priority Academic Program Development of Jiangsu Higher Education Institutions (PAPD), and the Program for Chang Jiang Scholars and Innovative Research Team in University (IRT_15R63).

Supplemental Material

Supplemental material for this article is available online.

ORCID iD

Jianguang Luo  <https://orcid.org/0000-0001-7852-8196>

References

1. Siegel R, Desantis C, Jemal A. Colorectal cancer statistics, 2014. *CA Cancer J Clin.* 2014;64:104-117.
2. Brenner H, Kloor M, Pox CP. Colorectal cancer. *Lancet.* 2014;383:1490-1502.
3. Zahreddine H, Borden KL. Mechanisms and insights into drug resistance in cancer. *Front Pharmacol.* 2013;4:28.
4. Hoa NT, Zhang JG, Delgado CL, et al. Human monocytes kill M-CSF-expressing glioma cells by BK channel activation. *Lab Invest.* 2007;87:115-129.
5. Sperandio S, de Belle I, Bredesen DE. An alternative, non-apoptotic form of programmed cell death. *Proc Natl Acad Sci U S A.* 2000;97:14376-14381.
6. Zhang C, Jiang Y, Zhang J, Huang J, Wang J. 8-p-hydroxybenzoyl tovarol induces paraptosis like cell death and protective autophagy in human cervical cancer HeLa cells. *Int J Mol Sci.* 2015;16:14979-14996.
7. Yoon MJ, Kang YJ, Lee JA, et al. Stronger proteasomal inhibition and higher CHOP induction are responsible for more effective induction of paraptosis by dimethoxycurcumin than curcumin. *Cell Death Dis.* 2014;5:e1112.
8. Wang WB, Feng LX, Yue QX, et al. Paraptosis accompanied by autophagy and apoptosis was induced by celastrol, a natural compound with influence on proteasome, ER stress and Hsp90. *J Cell Physiol.* 2012;227:2196-2206.
9. Lee D, Kim IY, Saha S, Choi KS. Paraptosis in the anti-cancer arsenal of natural products. *Pharmacol Ther.* 2016;162:120-133.
10. Li X, Weinman SA. Chloride channels and hepatocellular function: prospects for molecular identification. *Annu Rev Physiol.* 2002;64:609-633.
11. Diederich M, Cerella C. Non-canonical programmed cell death mechanisms triggered by natural compounds. *Semin Cancer Biol.* 2016;40-41:4-34.
12. Sawadogo WR, Schumacher M, Teiten MH, Dicato M, Diederich M. Traditional West African pharmacopeia, plants and derived compounds for cancer therapy. *Biochem Pharmacol.* 2012;84:1225-1240.
13. Cruz-Morales S, Castaneda-Gomez J, Rosas-Ramirez D, et al. Resin glycosides from ipomoea alba Seeds as potential chemosensitizers in breast carcinoma cells. *J Nat Prod.* 2016;79:3093-3104.
14. Pereda-Miranda R, Bah M. Biodynamic constituents in the Mexican morning glories: purgative remedies transcending boundaries. *Curr Top Med Chem.* 2003;3:111-131.
15. Pereda-Miranda R, Rosas-Ramirez D, Castaneda-Gomez J. Resin glycosides from the morning glory family. *Fortschr Chem Org Naturst.* 2010;92:77-153.
16. Rencurosi A, Mitchell EP, Cioci G, Perez S, Pereda-Miranda R, Imberty A. Crystal structure of tricolorin A: molecular rationale for the biological properties of resin glycosides found in some Mexican herbal remedies. *Angew Chem Int Ed Engl.* 2004;43:5918-5922.
17. Chen C, Ma T, Zhang C, et al. Down-regulation of aquaporin 5-mediated epithelial-mesenchymal transition and antimetastatic effect by natural product cairicoside E in colorectal cancer. *Mol Carcinog.* 2017;56:2692-2705.
18. Fan BY, Li ZR, Ma T, et al. Further screening of the resin glycosides in the edible water spinach and characterisation on their mechanism of anticancer potential. *J Funct Foods.* 2015;19:141-154.
19. Bai LJ, Luo JG, Chen C, Kong LY. Pharesinosides A-G, acylated glycosidic acid methyl esters derivatized by NH₂ silica gel on-column catalyzed from the crude resin glycosides of Pharbitis Semen. *Tetrahedron.* 2017;73:2863-2871.
20. Samadder P, Bittman R, Byun HS, Arthur G. A glycosylated antitumor ether lipid kills cells via paraptosis-like cell death. *Biochem Cell Biol.* 2009;87:401-414.
21. Wang L, Gundelach JH, Bram RJ. Cycloheximide promotes paraptosis induced by inhibition of cyclophilins in glioblastoma multiforme. *Cell Death Dis.* 2017;8:e2807.
22. Yoon MJ, Kim EH, Lim JH, Kwon TK, Choi KS. Superoxide anion and proteasomal dysfunction contribute to curcumin-induced paraptosis of malignant breast cancer cells. *Free Radic Biol Med.* 2010;48:713-726.
23. Peredamiranda R, Villatorovera R, Bah M, Lorence A. Pore-forming activity of morning glory resin glycosides in model membranes. *Rev Latinoamer Quím.* 2009:144-154.
24. Ono M, Noda N, Kawasaki T, Miyahara K. Resin glycosides. VII. Reinvestigation of the component organic and glycosidic

- acids of pharbitin, the crude ether-insoluble resin glycoside ("Convolvulin") of Pharbitidis Semen (seeds of *Pharbitis nil*). *Chem Pharm Bull (Tokyo)*. 1990;38:1892-1897.
25. Ono M, Takigawa A, Mineno T, et al. Acylated glycosides of hydroxy fatty acid methyl esters generated from the crude resin glycoside (pharbitin) of seeds of *Pharbitis nil* by treatment with indium(III) chloride in methanol. *J Nat Prod*. 2010;73:1846-1852.
 26. Bury M, Girault A, Megalizzi V, et al. Ophiobolin A induces paraptosis-like cell death in human glioblastoma cells by decreasing BKCa channel activity. *Cell Death Dis*. 2013;4:e561.
 27. Li B, Zhao J, Wang CZ, et al. Ginsenoside Rh2 induces apoptosis and paraptosis-like cell death in colorectal cancer cells through activation of p53. *Cancer Lett*. 2011;301:185-192.
 28. Edwards JC, Kahl CR. Chloride channels of intracellular membranes. *FEBS Lett*. 2010;584:2102-2111.